Organic & Biomolecular Chemistry

ROYAL SOCIETY OF CHEMISTRY

COMMUNICATION

View Article Online
View Journal | View Issue

Cite this: *Org. Biomol. Chem.*, 2025, **23**, 6360

Received 1st May 2025,
Accepted 14th June 2025

DOI: 10.1039/d5ob00717h

rsc.li/obc

Light-driven reductive cyclization catalyzed by vitamin B_{12}-based artificial photoenzymes†

Takumi Ogawa Ho,‡[a] Yi Ling Goh,‡[a] Wisely Chua,[b] Elaine Tiong,[b] Fong Tian Wong[b] and Zhennan Liu *[a,c]

In Nature, metabolically active vitamin B_{12} possesses an unusual metal–carbon bond that can be readily cleaved under visible light. This photolytic mechanism is crucial for B_{12}-dependent photoreceptors in regulating the gene expression in microbes, but no enzymes have been identified so far that exploit the unique photoreactivity of cobalamin. Here, we present the assembly of cobalamin–serum albumin conjugates and demonstrate their use as artificial photoenzymes to catalyze the intramolecular cyclization of unactivated alkyl halides with tethered alkenes. The encapsulation of cobalamin within a protein environment enables the reaction to occur with 4.5 × enhanced reactivity for the model substrate. A range of alkyl halides were successfully cyclized under the developed conditions to produce various molecular scaffolds and a tandem Giese reaction with methyl acrylate was also demonstrated.

Vitamin B_{12} is a unique class of naturally occurring organometallic complexes that are found as essential cofactors for numerous biological processes.[1,2] These complexes contain a cobalt ion surrounded by a corrin ring and coordinated with a nitrogen atom from dimethylbenzimidazole that is covalently appended to the corrin (Fig. 1a). With a variable sixth ligand, native vitamin B_{12} exists in metabolically active forms as adenosylcobalamin (AdoCbl, **1a**) and methylcobalamin (MeCbl, **1b**).[3] These alkylcobalamins possess fairly weak Co–C bonds that can readily undergo homolytic or heterolytic scissions. Natural enzymes effectively exploit this feature in distinct reaction pathways and catalyze a range of molecular transformations, including rearrangement, methylation, and dehalogenation.[4] For instance, the isomerization catalyzed by AdoCbl-dependent enzymes is initiated by homolytic cleavage of the Co–C bond, generating Co(II) and an adenosyl radical

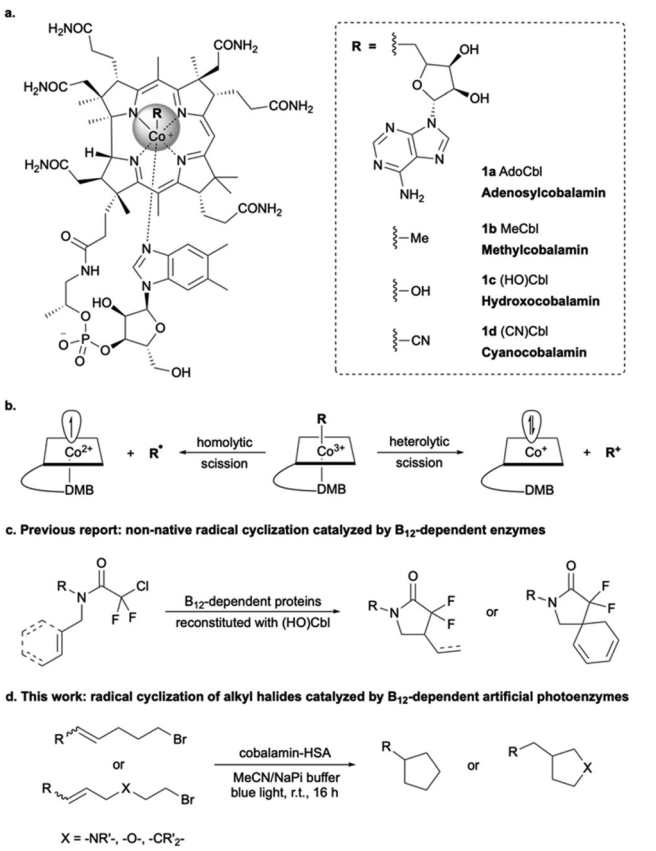

Fig. 1 (a) Structures of cobalamin derivatives (**1a–1d**). (b) Two different modes of Co–C bond cleavage. (c) Previously reported non-native radical cyclization catalyzed by reconstituted B_{12}-dependent enzymes. (d) This work: light-driven radical cyclization of alkyl halides catalyzed by cobalamin-dependent artificial photoenzymes.

[a]*Institute of Sustainability for Chemicals, Energy and Environment (ISCE²), Agency for Science, Technology and Research (A*STAR), 8 Biomedical Grove, Neuros #07-01, Singapore 138665, Republic of Singapore. E-mail: e1347801@u.duke.nus.edu*
[b]*Institute of Molecular and Cell Biology (IMCB), Agency for Science, Technology and Research (A*STAR), 61 Biopolis Drive, Proteos #07-01, Singapore 138673, Republic of Singapore*
[c]*Duke-NUS Medical School, 8 College Rd, Singapore 169857, Republic of Singapore*
†Electronic supplementary information (ESI) available. See DOI: https://doi.org/10.1039/d5ob00717h
‡These authors contributed equally to this work.

that can abstract a hydrogen atom from the substrate and facilitate the rearrangement of the carbon skeleton (Fig. 1b).[5,6] In contrast, the Co–C bond in some MeCbl-dependent enzymes undergoes heterolytic cleavage, transferring the methyl group to the substrate and generating a Co(I) species that is known as a "supernucleophile" (Fig. 1b).[7,8]

The unique redox chemistry of cobalt corrinoids, combined with their non-toxic nature and abundance as natural catalysts, has captured the interests of synthetic chemists, leading to the application of cobalamin catalysts in a range of synthetically valuable transformations, including dehalogenation, dimerization, cyclopropanation, and radical addition to unsaturated bonds.[9–11] Hydrophobic derivatives of cobalamin have also been developed to extend their applications to a broader range of organic solvents.[12,13] However, most of the reaction conditions involving cobalamins and their derivatives are far from being green due to the need of polar organic solvents, and the extra synthetic efforts required for preparing cobalamin derivatives negate their advantage of being a natural catalyst. Given the mounting concerns about the environmental impact of chemical manufacturing processes, it is important to develop greener methodologies that utilize the native forms of vitamin B_{12} in environmentally benign solvents, ideally in water and with low catalyst loading.

Introducing organometallic complexes into proteins to create artificial metalloenzymes has recently emerged as a promising strategy to impart new-to-nature reactivity to biocatalysts and enable transition metal-catalyzed reactions to take place in aqueous environments under mild conditions.[14–16] Lewis *et al.* have recently reported that vitamin B_{12}-dependent proteins could be reconstituted with hydroxocobalamin (**1c**) to catalyze non-native reactions including C–H alkylation of styrene,[17] *N*-alkylation of aniline[18] and intramolecular radical cyclization of a series of α-chloroacetamides (Fig. 1c).[19] However, to the best of our knowledge, the chemical processes catalyzed by natural or reconstituted cobalamin-containing enzymes reported to date remain thermally driven, despite the known photoactivity of cobalamin.[9–11]

The first evidence of cobalamin being used as a photoreactive cofactor in nature was reported in 2011.[20–22] CarH, an AdoCbl-dependent photoreceptor in Myxobacteria, was found to be regulated by light. Upon light excitation, AdoCbl undergoes photolysis, and the dissociation of the adenosyl radical triggers a protein conformational change that subsequently activates carotenoid gene expression. The discovery of CarH has led to the identification of a whole new family of photoreceptor proteins that use cobalamin as a chromophore,[23,24] but no photoenzymes of this type have been found so far.

Driven by the goal of harnessing the versatile catalytic reactivity of cobalamins and integrating it into nature's biocatalyst repertoire for the advancement of sustainable manufacturing processes, we envisaged to develop a cobalamin-containing artificial photoenzyme that can catalyze synthetically desirable reactions with light as the ultimate source of energy. In order to create the artificial photoenzyme, we selected human serum albumin (HSA) as a host for cyanocobalamin (CNCbl **1d**, a commercially manufactured form of vitamin B_{12}). Serum albumins are highly abundant proteins found in blood plasma, serving as transporters for a diverse range of compounds. Known for their robustness, commercial availability, and ease of handling, serum albumins have been widely used as protein hosts for the preparation of artificial metalloenzymes.[25–28] By incorporating CNCbl within a chiral protein matrix,[29] it holds the promise of solubilizing organic substrates, inducing asymmetry, and enabling photocatalysis to occur in aqueous media. We hereby present the assembly of cobalamin–serum albumin conjugates and their application as a photobiocatalyst for reductive cyclization reactions (Fig. 1d).

Radical cyclization reactions can rapidly assemble molecules with high structural complexity from simple starting materials. In these reactions, a highly reactive radical intermediate triggers the sequential formation and breakage of multiple bonds in much the same way as Nature constructs polycyclic terpenes and steroids.[30,31] Using alkyl halides as starting materials, we envisioned that the "supernucleophilic" reactivity of Co(I) would facilitate the dehalogenation of alkyl halides to form Co(III)–carbon bonds. The photolytic cleavage of the resulting alkylated intermediate would then generate carbon-centered radicals that could add to a tethered alkene group to construct new carbocycles (ESI Fig. 1†).

Based on this hypothesis, exploratory experiments were carried out with CNCbl–HSA conjugates and the alkyl bromide **2** was selected as a model substrate. In the presence of a bio-

Table 1 Screening of photochemical conditions for intramolecular cyclization of **2**[a]

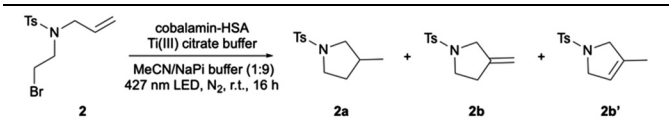

2 **2a** **2b** **2b'**

Entry	Deviation from standard conditions	Yield of **2a**[b]	Yield of **2b**[b]
1	None	77%	2%
2[c]	CNCbl, $NaBH_4$, MeCN	9%	14%
3[d]	CNCbl, Zn, MeOH	42%	n.d.[e]
4	CNCbl only (no HSA)	17%	4%
5	HSA only (no CNCbl)	n.d.	n.d.
6	Under dark	n.d.	n.d.
7	390 nm	44%	<2%
8	440 nm	46%	<2%
9	Ti(III) citrate/NaPi buffer (pH 6.0)	27%	5%
10	Ti(III) citrate/NaPi buffer (pH 7.0)	60%	3%

[a] Standard conditions: **2** (0.020 mmol), CNCbl (0.18 mol%), HSA (0.36 mol%), Ti(III) citrate (66 mM), MeCN (0.20 mL), NaPi buffer (100 mM, pH 8.0, 1.8 mL), 427 nm, N_2, r.t., 16 h. [b] The yields were determined by ^{1}H NMR using 1,3,5-trimethoxybenzene as an internal standard. The biocatalytic reactions were performed as individual duplicates and the data represent the average from duplicates. n.d. = not detected. [c] Conditions: **2** (0.20 mmol), CNCbl (5.0 mol%), $NaBH_4$ (6.0 equiv.), $NaHCO_3$ (1.2 equiv.), MeCN (2.0 mL), 390 nm, N_2, r.t., 16 h. [d] Conditions: **2** (0.20 mmol), CNCbl (5.0 mol%), Zn dust (6.0 equiv.), NH_4Cl (3.5 equiv.), MeOH (2.0 mL), 390 nm, N_2, r.t., 16 h. [e] The internal alkene **2b'** was formed as a side product with 6% yield.

compatible reductant, Ti(III) citrate, and light irradiation at 427 nm, the CNCbl–HSA hybrid furnished the formation of pyrrolidine **2a** with a yield of 77%, while producing negligible amount of alkene side products (**2b** and **2b′**) (Table 1, entry 1). The model substrate was also tested under two reported conditions for CNCbl-catalyzed dehalogenation in organic solvents.[32,33] Using $NaBH_4$ as the reductant and MeCN as the solvent, the pyrrolidine products (**2a** and **2b**) were obtained in low yields (Table 1, entry 2), while the major product resulted from dehalogenation of the starting material. When Zn was used as the reductant in MeOH, **2b** was formed with 42% yield, along with a trace amount of the internal alkene product **2b′** (Table 1, entry 3). Control experiments were conducted with CNCbl alone, resulting in only 17% yield of the pyrrolidine product **2a** (Table 1, entry 4). When either cobalamin or light was omitted from the reaction, no products were observed (Table 1, entries 5 and 6). We also screened various wavelengths of light and different pH levels for the reaction buffer, and found that the irradiation at 427 nm and a buffer pH of 8.0 yielded the optimal result (Table 1, entries 7–10).

Having determined the enhanced photocatalytic reactivity of cobalamin within a protein environment, we proceeded to evaluate other commercially available serum albumins as potential hosts for CNCbl, including bovine serum albumin (BSA), rabbit serum albumin (RbSA), porcine serum albumin (PSA), sheep serum albumin (SSA), and rat serum albumin (RtSA), in the reductive cyclization of **2**. Table 2 demonstrates that BSA was nearly as effective as HSA, yielding 68% of the pyrrolidine product **2a** (Table 2, entry 1), whereas the CNCbl–RtSA conjugate showed minimal enhancement in reaction yield compared to the unbound cobalamin (Table 2, entry 5).

It has been reported that some natural vitamin B_{12}-dependent proteins could catalyze non-native cyclization reactions after reconstitution with (OH)Cbl.[19] To evaluate whether these natural cobalamin hosts offer a better platform than serum albumin for constructing a photoenzyme that facilitates photocyclization reactions, we expressed three proteins, DhaF4611, CarH and MtaC, reconstituted them with CNCbl, and tested their reactivity in the cyclization of model substrate **2**. For the photocyclization catalyzed by the three reconstituted proteins, similar levels of pyrrolidine product **2a** were obtained (29–32%), but significant amounts of alkene side product **2b** were also formed (Table 3, entries 1–3). The reaction catalyzed by reconstituted DhaF4611 demonstrated the highest selectivity for alkane formation over the alkene side product; however, its overall yield and selectivity did not surpass those of the CNCbl–HSA conjugate (Table 3, entry 1).

We then aimed to expand the substrate scope for intramolecular cyclization reactions catalyzed by CNCbl–HSA conjugate. By modifying the leaving group of the model substrate **2**, we observed that the reaction proceeded less efficiently with a chloride group, yielding only trace amounts of the cyclization product (Table 4, entry 1). In contrast, substituting bromide with iodide as the leaving group led to a significantly higher yield of the cyclization product (87%) and only trace amounts of the alkene side product (Table 4, entry 2). In addition, the photocyclization of **4** could be scaled up to 0.4 mmol, achieving an isolated yield of 66%. However, no products were obtained with a tosyl leaving group (Table 4, entry 3). The CNCbl–HSA also catalyzed the formation of five-membered carbocyclic products from different malonate derivatives. The cyclization of dimethyl malonate **6** proceeded smoothly with a yield of 53%, while the introduction of a phenyl substituent on the allyl group of malonate derivative **7** reduced the yield of the cyclized product to 19% (Table 4, entries 4 and 5). The methodology was further evaluated for its synthetic potential in three different bicyclic structures. Upon exposure to light, hexahydrofuro[2,3-*b*]furan **8a** was exclusively formed from tetrahydrofuran derivative **8** with a yield of 46% (Table 1, entry 6). Another fused bicyclic structure, pyrrolizidinone (**9a** and **9b**), was obtained from γ-lactam derivative **9** with 43% yield and a diastereomeric ratio of 2.6 : 1 (Table 4, entry 7). The reductive cyclization of 3-substituted cyclohexenone derivative **10** produced spirocycle **10a** with 60% yield, and the competing dehydrobromination formed the side product **10b** in 9% yield (Table 4, entry 8). Attempts to synthesize spirocycles from cyclohexenone derivative **11** were unsuccessful, yielding primarily the debrominated product **11a** (Table 4, entry 9). Similarly, the predominant formation of debrominated product from styrene derivative **12** shows that the photocyclization follows a 5-*exo-trig* pathway (Table 4, entry 10).

Table 2 Intramolecular cyclization of **2** catalyzed by various cobalamin–serum albumin conjugates[a]

Entry	Source serum albumins	Yield of **2a**[b]	Yield of **2b**[b]
1	Bovine	68%	<2%
2	Rabbit	52%	<2%
3	Porcine	25%	<2%
4	Sheep	54%	<2%
5	Rat	22%	<1%

[a] The reactions were carried out under the standard conditions specified in Table 1. [b] The yields were determined by ^{1}H NMR using 1,3,5-trimethoxybenzene as an internal standard, with the data representing averages from duplicate experiments.

Table 3 Intramolecular cyclization of **2** catalyzed by natural B_{12}-dependent proteins reconstituted with CNCbl[a]

Entry	B_{12}-dependent proteins	Yield of **2a**[b]	Yield of **2b**[b]
1	DhaF4611	32%	14%
2	CarH	31%	29%
3	MtaC	29%	38%

[a] Standard conditions: **2a** (0.020 mmol), B_{12}-dependent proteins (0.16 mol%), Ti(III) citrate (66 mM), MeCN (0.20 mL), NaPi buffer (100 mM, pH 8.0, 1.8 mL), 427 nm, N_2, r.t., 16 h. [b] The yields were determined by ^{1}H NMR using 1,3,5-trimethoxybenzene as an internal standard. The biocatalytic reactions were performed as individual duplicates and the data represent the average from duplicates.

Table 4 Intramolecular cyclization of alkyl halides catalyzed by CNCbl–HSA conjugates[a]

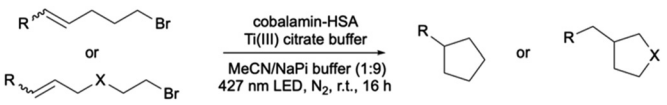

Entry	Substrate	Product		Yield[b]
1	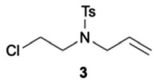 **3**	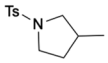 **2a**	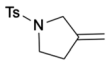 **2b**	**2a:** 4% **2b:** n.d.
2	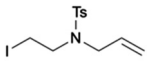 **4**	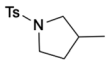 **2a**	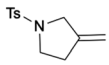 **2b**	**2a:** 87% **2b:** 3%
3	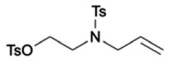 **5**	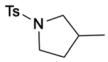 **2a**	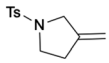 **2b**	No reaction
4	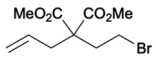 **6**	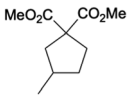 **6a**	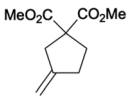 **6b**	**6a:** 53% **6b:** 3%
5	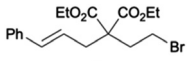 **7**	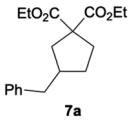 **7a**		**7a:** 19%
6	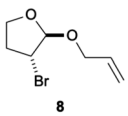 **8**	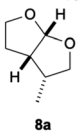 **8a**		**8a:** 46%
7	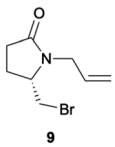 **9**	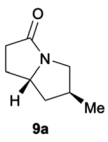 **9a**	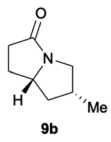 **9b**	**9a:** 31% **9b:** 12%
8	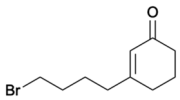 **10**	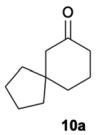 **10a**	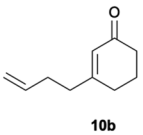 **10b**	**10a:** 60% **10b:** 9%
9	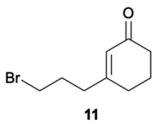 **11**	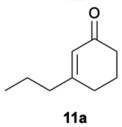 **11a**	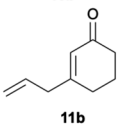 **11b**	**11a:** 77% **11b:** 9%
10	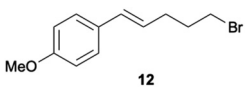 **12**	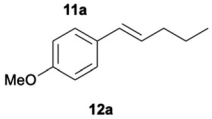 **12a**	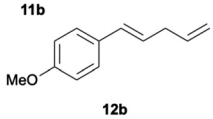 **12b**	**12a:** 20% **12b:** 9%

[a] Standard conditions: alkyl halides (0.020 mmol), CNCbl (0.18 mol%), HSA (0.36 mol%), Ti(III) citrate (66 mM), MeCN (0.20 mL), NaPi buffer (100 mM, pH 8.0, 1.8 mL), 427 nm, N_2, r.t., 16 h. [b] The yields were determined by ^{1}H NMR using 1,3,5-trimethoxybenzene as an internal standard. The biocatalytic reactions were performed as individual duplicates and the data represent the average from duplicates. n.d. = not detected.

Along the line, we further investigated the potential application of the photoenzyme in difunctionalization of alkenes. By incorporating an electron-deficient alkene, such as methyl acrylate, into the reaction, it is possible to trap the cyclized intermediate, form additional C–C bonds and expand the scope of possible transformations. Three different ratios of **2** : methyl acrylate were tested and a ratio of 1 : 3 provided the highest yield of the difunctionalized products, **13a** and **13b** from mono- and di-addition of methyl acrylate (Table 5, entries 1, 2 and 4). Increasing the concentration of titanium citrate could further improve the yield to 63% (Table 5, entry 3). Although the production of **13a** and **13b** is not yet selective at this stage, this strategy still holds promise for broader applications in alkene functionalization with further optimization.

Table 5 Tandem Giese reaction catalyzed by CNCbl–HSA conjugates[a]

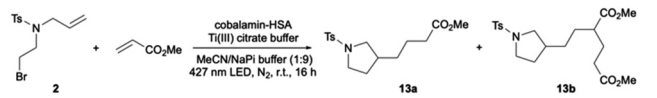

Entry	2 (mmol)	Methyl acrylate (mmol)	Yield of (**13a** + **13b**)[b]	Unreacted substrate[b]
1	0.02	0.02	28%	74%
2	0.02	0.06	51%	52%
3[c]	0.02	0.06	63%	40%
4	0.02	0.20	38%	62%

[a] Standard conditions: **2** (0.020 mmol), methyl acrylate (1.0, 3.0 or 10 equiv.), CNCbl (0.18 mol%), HSA (0.36 mol%), Ti(III) citrate (66 mM), MeCN (0.20 mL), NaPi buffer (100 mM, pH 8.0, 1.8 mL), 427 nm, N_2, r. t., 16 h. [b] The yields were determined by ^{1}H NMR using 1,3,5-trimethoxybenzene as an internal standard. The biocatalytic reactions were performed as individual duplicates and the data represent the average from duplicates. [c] 110 mM Ti(III) citrate was used.

Conclusions

In this work, we developed a novel class of artificial photoenzymes by incorporating photoreactive cyanocobalamin into the robust protein scaffold of human serum albumin. The resulting photoenzyme exhibited significantly enhanced catalytic efficiency, enabling the intramolecular radical cyclization of alkyl bromides with much higher yields than cobalamin alone. The synthetic utility of the photoenzyme was demonstrated through moderate to good yields across a range of substrates and the formation of three distinct bicyclic structures with enhanced complexity. The reaction system could be further tailored by introducing an electron-deficient alkene, allowing a tandem Giese reaction to occur and facilitating the formation of difunctionalized products of alkenes. The development of such a photoreactive catalytic system from cyanocobalamin and serum albumin allows for the synthesis of complex molecular structures using light as the ultimate energy source under environmental-friendly conditions. This strategy is expected to offer a sustainable approach to accessing complex carbocycles in the future.

Author contributions

Takumi Ogawa Ho: Methodology, validation, investigation, writing – review and editing; Goh Yi Ling: Validation, investigation, resources, writing – review and editing; Wisely Chua: Resources; Elaine Tiong: Resources; Fong Tian Wong: Writing – review and editing, supervision, funding acquisition; Zhennan Liu: Conceptualization, methodology, writing – original draft, supervision, funding acquisition.

Conflicts of interest

There are no conflicts to declare.

Data availability

The data supporting this article have been included as part of the ESI.†

Acknowledgements

This research is supported by Manufacturing, Trade and Connectivity (MTC) under its RIE2025 Young Individual Research Grants (M22K3c0099), and Agency for Science, Technology and Research (A*STAR) under its Career Development Fund (C210812022).

References

1 K. Gruber, B. Puffer and B. Kräutler, *Chem. Soc. Rev.*, 2011, **40**, 4346–4363.
2 B. Kräutler, in *Water Soluble Vitamins: Clinical Research and Future Application*, ed. O. Stanger, Springer Netherlands, Dordrecht, 2012, pp. 323–346. DOI: **10.1007/978-94-007-2199-9_17**.
3 J. Bridwell-Rabb and C. L. Drennan, *Curr. Opin. Chem. Biol.*, 2017, **37**, 63–70.
4 R. Banerjee and S. W. Ragsdale, *Annu. Rev. Biochem.*, 2003, **72**, 209–247.
5 G. H. Reed, *Curr. Opin. Chem. Biol.*, 2004, **8**, 477–483.
6 K. R. Wolthers, S. E. J. Rigby and N. S. Scrutton, *J. Biol. Chem.*, 2008, **283**, 34615–34625.
7 R. G. Matthews, *Acc. Chem. Res.*, 2001, **34**, 681–689.
8 R. G. Matthews, M. Koutmos and S. Datta, *Curr. Opin. Struct. Biol.*, 2008, **18**, 658–666.
9 M. Giedyk, K. Goliszewska and D. Gryko, *Chem. Soc. Rev.*, 2015, **44**, 3391–3404.
10 T. Wdowik and D. Gryko, *ACS Catal.*, 2022, **12**, 6517–6531.
11 M. Giedyk and D. Gryko, *Chem Catal.*, 2022, **2**, 1534–1548.
12 Y. Hisaeda, K. Tahara, H. Shimakoshi and T. Masuko, *Pure Appl. Chem.*, 2013, **85**, 1415–1426.
13 K. Ó. Proinsias, M. Giedyk and D. Gryko, *Chem. Soc. Rev.*, 2013, **42**, 6605–6619.
14 F. Schwizer, Y. Okamoto, T. Heinisch, Y. Gu, M. M. Pellizzoni, V. Lebrun, R. Reuter, V. Köhler, J. C. Lewis and T. R. Ward, *Chem. Rev.*, 2018, **118**, 142–231.
15 H. J. Davis and T. R. Ward, *ACS Cent. Sci.*, 2019, **5**, 1120–1136.
16 B. Large, N. G. Baranska, R. L. Booth, K. S. Wilson and A.-K. Duhme-Klair, *Curr. Opin. Green Sustainable Chem.*, 2021, **28**, 100420.
17 X. Yang, B. H. R. Gerroll, Y. Jiang, A. Kumar, Y. S. Zubi, L. A. Baker and J. C. Lewis, *ACS Catal.*, 2022, **12**, 935–942.
18 A. Kumar, X. Yang, J. Li and J. C. Lewis, *Chem. Commun.*, 2023, **59**, 4798–4801.
19 J. Li, A. Kumar and J. C. Lewis, *Angew. Chem., Int. Ed.*, 2023, **62**, e202312893.

20 J. M. Ortiz-Guerrero, M. C. Polanco, F. J. Murillo, S. Padmanabhan and M. Elías-Arnanz, *Proc. Natl. Acad. Sci. U. S. A.*, 2011, **108**, 7565–7570.
21 R. J. Kutta, S. J. O. Hardman, L. O. Johannissen, B. Bellina, H. L. Messiha, J. M. Ortiz-Guerrero, M. Elías-Arnanz, S. Padmanabhan, P. Barran, N. S. Scrutton and A. R. Jones, *Nat. Commun.*, 2015, **6**, 7907.
22 H. Poddar, R. Rios-Santacruz, D. J. Heyes, M. Shanmugam, A. Brookfield, L. O. Johannissen, C. W. Levy, L. N. Jeffreys, S. Zhang, M. Sakuma, J.-P. Colletier, S. Hay, G. Schirò, M. Weik, N. S. Scrutton and D. Leys, *Nat. Commun.*, 2023, **14**, 5082.
23 S. Padmanabhan, M. Jost, C. L. Drennan and M. Elías-Arnanz, *Annu. Rev. Biochem.*, 2017, **86**, 485–514.
24 S. Padmanabhan, R. Pérez-Castaño and M. Elías-Arnanz, *Curr. Opin. Struct. Biol.*, 2019, **57**, 47–55.
25 M. T. Reetz and N. Jiao, *Angew. Chem., Int. Ed.*, 2006, **45**, 2416–2419.
26 J. Tang, F. Huang, Y. Wei, H. Bian, W. Zhang and H. Liang, *Dalton Trans.*, 2016, **45**, 8061–8072.
27 J. Tang, P. Yao, L. Wang, H. Bian, M. Luo and F. Huang, *RSC Adv.*, 2018, **8**, 40720–40730.
28 T.-C. Chang, K. Vong, T. Yamamoto and K. Tanaka, *Angew. Chem., Int. Ed.*, 2021, **60**, 12446–12454.
29 H.-N. Hou, Z.-D. Qi, Y.-W. OuYang, F.-L. Liao, Y. Zhang and Y. Liu, *J. Pharm. Biomed. Anal.*, 2008, **47**, 134–139.
30 K. J. Romero, M. S. Galliher, D. A. Pratt and C. R. J. Stephenson, *Chem. Soc. Rev.*, 2018, **47**, 7851–7866.
31 J. Liao, X. Yang, L. Ouyang, Y. Lai, J. Huang and R. Luo, *Org. Chem. Front.*, 2021, **8**, 1345–1363.
32 S. Smoleń, A. Wincenciuk, O. Drapała and D. Gryko, *Synthesis*, 2020, 1645–1653.
33 R. Bam, A. S. Pollatos, A. J. Moser and J. G. West, *Chem. Sci.*, 2021, **12**, 1736–1744.